Joint Detection of Primary Systems Using UWB Impulse Radios

Serhat Erküçük, *Member, IEEE,* Lutz Lampe, *Senior Member, IEEE,* and Robert Schober, *Fellow, IEEE*

***Abstract*—Regulation in Europe and Japan requires the implementation of detect-and-avoid (DAA) techniques in some bands for the coexistence of licensed primary systems and secondary ultra wideband (UWB) systems. In a typical coexistence scenario, a primary system may have potentially interdependent uplink-downlink communication channels (e.g., simultaneous uplink-downlink communications in a frequency division duplex system) overlapping with the frequency band of a UWB system. If such interdependencies of primary systems' activities are known, the UWB system's ability to detect primary systems can be improved. In this study, we are interested in determining the possible gains in the detection performance when taking interdependencies into account for practically implementable detection methods. Contrary to selecting the detection thresholds individually for each band as in a conventional detection approach, the bands are jointly processed. To this end, maximum a posteriori (MAP) decision variables are generated at the receiver, and bias terms are introduced to achieve a desired trade-off between the probabilities of detection and false alarm. In addition to finding the optimal detection results based on the Neyman-Pearson (NP) test, a suboptimal but practically implementable approach is also considered, and the gain compared to conventional independent detection is quantified for various practical scenarios. The results obtained from this study can be used for improving the primary system detection performance of UWB systems, as well as for cognitive radios that perform spectrum sensing in multiple bands.**

***Index Terms*—Ultra wideband (UWB) systems, detect-and-avoid (DAA), coexistence, spectrum sensing, joint detection, cognitive radios.**

I. Introduction

DESPITE the low transmission power of underlay ultra wideband (UWB) systems [1], regulatory agencies in Europe and Japan have made the implementation of detect-and-avoid (DAA) techniques mandatory in some bands to avoid interference to existing systems [2]. In any DAA technique, the first step is *spectrum sensing*, which has been widely explored in the context of cognitive radios [3] – [5]. Recently, there have been spectrum sensing studies for low-rate UWB impulse radios (UWB-IRs) for DAA purposes [6], [7]. The common characteristics of the methods in [3] – [7] are the detection of a primary system in a *single frequency band* and the improvement of the detection performance via *cooperative techniques*. While cooperative techniques are necessary to achieve a high level of signal detection reliability, signal detection in a single frequency band should be extended to multiple frequency bands if multiple bands are occupied by licensed systems within the bandwidth of a UWB system.

The literature on energy detection in multiple frequency bands is rather limited compared to energy detection in a single band. In [8], we studied the energy detection of multiple primary systems operating in the same frequency band as UWB-IRs, where each system was assumed to access the channel independently. In [9], multiband joint detection for cognitive radios was considered, where the aggregate opportunistic throughput was maximized. The common assumption in [8] and [9] is that the primary systems in different bands are *independent*. However, in some practical scenarios the licensed systems in different bands may be dependent. For example, the presence of an active uplink could possibly mean there is also an active downlink.

In this study, the primary system detection performance of UWB-IR systems is investigated assuming that the primary systems are potentially dependent (e.g., frequency division duplex (FDD) uplink-downlink communications, etc.). To the best of our knowledge, we are the first to consider *interdependencies between primary systems' activities* in multiband spectrum sensing problems. We are particularly interested in (i) determining possible gains in detection performance when taking interdependencies into account, and (ii) employing practical methods for implementation. To this end, we consider processing the bands jointly based on the maximum a posteriori (MAP) decision rule and compare the detection performance with conventional independent detection. For joint detection, the optimum detection results are obtained based on the Neyman-Pearson (NP) test. Also, a suboptimal but practically implementable approach with near-optimum performance is proposed. The detection gains are quantified in terms of the primary system interdependence, signal-to-noise-ratio (SNR), and energy integration time in each band for practical scenarios.

The rest of the paper is organized as follows. In Section II, the system model is presented. In Section III, the joint detection method based on MAP detection is introduced. In Section IV, numerical results are presented, and concluding remarks are given in Section V.

II. System Model

We initially consider the general case of M primary systems coexisting with a UWB-IR system in the same frequency band. Later on, we will focus on the practically relevant case of detection of an FDD uplink-downlink system.

Manuscript received June 7, 2010; revised November 25, 2010; accepted November 28, 2010. The associate editor coordinating the review of this letter and approving it for publication was L. Yang.

This research was supported in part by a Marie Curie International Reintegration Grant within the 7^{th} European Community Framework Programme, and by the National Sciences and Engineering Research Council of Canada (STPGP 364995-08). Part of this work was presented at the IEEE International Conference on Ultra Wideband, Vancouver, BC, Canada, Sep. 2009.

S. Erküçük is with the Department of Electronics Engineering, Kadir Has University, Cibali, 34083, Istanbul, Turkey (e-mail: serkucuk@khas.edu.tr).

L. Lampe and R. Schober are with the Department of Electrical and Computer Engineering, University of British Columbia, Vancouver, BC V6T 1Z4, Canada (e-mail: {lampe, rschober}@ece.ubc.ca).

Digital Object Identifier 10.1109/TWC.2011.122010.100990

A. UWB-IR Receiver Model

It is assumed that the UWB-IR system has prior knowledge of the carrier frequencies and transmission bandwidths of the primary systems, and an ideal zonal bandpass filter, $h_{ZF,m}(t)$, centered at f_m and with bandwidth W_m, is employed before energy detection is performed. Accordingly, the signal received in the mth frequency band after filtering is given by

$$r_m(t) = A_m\, e^{j\theta_m}\, s_m(t-\tau_m) + n_m(t), \quad 1 \le m \le M, \quad (1)$$

where $s_m(t)$ is the primary signal passing through a channel[1] with amplitude A_m and phase θ_m uniformly distributed over $[0, 2\pi)$ [8], τ_m is the timing offset between the two systems, and $n_m(t)$ is band-limited additive white Gaussian noise (AWGN) with variance $\sigma^2_{n_m} = N_0 W_m$. Using a square-law detector and normalizing the output with the two-sided noise power spectral density $N_0/2$, the decision variable for the mth system can be obtained as $d_m = \frac{2}{N_0}\int_0^{T_m} |r_m(t)|^2\, dt$, where T_m is the integration time for the mth system and $|\cdot|$ is the absolute value operator. Adopting the sampling theorem approximation used for bandpass signals in [3], the decision variable can be approximated as

$$d_m \approx \frac{1}{N_0 W_m} \sum_{i=1}^{T_m W_m} \Big[(A_c s_{ci} - A_s s_{si} + n_{ci})^2 + (A_c s_{si} + A_s s_{ci} + n_{si})^2\Big], \quad (2)$$

where s_{ci} and n_{ci} (s_{si} and n_{si}) are the in-phase (quadrature) components of $s_m(t-\tau_m)$ and $n_m(t)$ sampled at the Nyquist rate, $A_c = A_m \cos\theta_m$, and $A_s = A_m \sin\theta_m$.

B. Hypotheses and Performance Measures

We now define two hypotheses, $H_{0,m}$ and $H_{1,m}$, corresponding to the absence and presence of the signal of the mth primary system as

$$H_{0,m}: \quad r_m(t) = n_m(t) \quad (3)$$

$$H_{1,m}: \quad r_m(t) = A_m\, e^{j\theta_m}\, s_m(t-\tau_m) + n_m(t). \quad (4)$$

Under $H_{0,m}$, it can be shown based on (2) that d_m has a χ^2 distribution with $N_m = 2T_m W_m$ degrees of freedom (DOF) and variance $\sigma^2_m = \frac{\sigma^2_{n_m}}{N_0 W_m} = 1$. Under $H_{1,m}$, based on the central limit theorem, the samples of a primary signal given in (2) for a large number of subcarriers K sampled at the Nyquist rate can be approximated as independent and identically distributed (i.i.d.) zero mean Gaussian random variables. Accordingly, when the primary system is active, d_m has a χ^2 distribution with $N_m = 2T_m W_m$ DOF and variance $\sigma^2_m = \gamma_m + 1$, where $\gamma_m = \frac{A_m^2 \sigma_s^2}{N_0 W_m}$ is the SNR, σ_s^2 is the variance of the primary signal samples, and the term "1" is due to the normalized noise samples. Thus, the probability density function (pdf) of d_m for either hypothesis can be expressed as

$$f_{D_m}(d_m) = \frac{1}{\sigma_m^{N_m}\, 2^{N_m/2}\, \Gamma(N_m/2)}\, d_m^{N_m/2-1} e^{-d_m/2\sigma^2_m}, \quad (5)$$

where $\Gamma(a,b) = \int_b^\infty e^{-t} t^{a-1} dt$ is the upper incomplete Gamma function and $\Gamma(a) = \Gamma(a,0)$ is the Gamma function [10]. To decide on the absence or presence of the mth primary system, the UWB-IR receiver compares the decision variable d_m to a pre-selected threshold value λ_m in order to take an action. The performance measures, probability of false alarm and probability of detection, for the mth system can be expressed as

$$P_{f,m} = \Pr[d_m > \lambda_m | H_{0,m}] \text{ and } P_{d,m} = \Pr[d_m > \lambda_m | H_{1,m}], \quad (6)$$

respectively. Based on (5) both probabilities can be obtained as

$$P_{x,m} = Q\left(\frac{N_m}{2}, \frac{\lambda_m}{2\sigma_m^2}\right) = \frac{\Gamma\left(\frac{N_m}{2}, \frac{\lambda_m}{2\sigma_m^2}\right)}{\Gamma\left(\frac{N_m}{2}\right)}, \; x \in \{f, d\}, \quad (7)$$

with the corresponding σ_m^2 values for $H_{0,m}$ and $H_{1,m}$, where $Q(a,b)$ is the regularized upper incomplete Gamma function [10]. By adjusting the threshold value λ_m, desired $(P_{f,m}, P_{d,m})$-pairs can be obtained for given σ_m^2 and N_m values.

C. Hypotheses for Multiple Systems

In the presence of multiple systems, the hypotheses have to be redefined. Initially, the set of hypotheses for M systems is defined as $\mathbf{H} = \left\{\left[H_{x_M,M}, \ldots, H_{x_2,2}, H_{x_1,1}\right] | \, x_m \in \{0,1\}\right\}$ with 2^M possible hypothesis vectors. We then define $\mathbf{H}_0 \in \mathbf{H}$, where $x_m = 0$, $\forall m$, for the case when no primary system is active, and $\mathbf{H}_1 \in \mathbf{H}$ for the remaining $2^M - 1$ cases when at least one system is active. This means that the UWB-IR system can safely transmit when $\mathbf{H}_0$ holds, and has to take precautions in the case of $\mathbf{H}_1$. We further define $\mathbf{H}_{1,i}$, $1 \le i \le 2^M - 1$, where

$$(i)_{10} = (x_M \cdots x_2\, x_1)_2, \quad (8)$$

$(\cdot)_n$ is the logarithmic base n (e.g., $(3)_{10} = (1\,1)_2$ when $M = 2$), $\{x_m, \forall m\}$ refer to the subscripts of $\{H_{x_m,m}\}$, and $\mathbf{H}_1 = \bigcup_{i=1}^{2^M-1} \mathbf{H}_{1,i}$.

D. Joint System Activity Values

We now introduce the joint system activity values $\mathbf{p} = [p_0\; p_1\; \ldots\; p_i\; \ldots\; p_{2^M-1}]$, which provide information about the interdependencies of the primary systems. We define $p_0 = \Pr[\mathbf{H}_0]$ as the probability that no primary system is active, and $p_i = \Pr[\mathbf{H}_{1,i}]$, $1 \le i \le 2^M - 1$, as the probability that $\mathbf{H}_{1,i}$ holds,[2] where $\sum_{i=0}^{2^M-1} p_i = 1$. For the special case of an FDD uplink-downlink communication system (i.e., $M = 2$), the system is inactive if both links are inactive. On the other hand, if either link or both of the links are active, then the system is active. In Section IV, the effect of the values of $\{p_i\}$ on the detection performance will be elaborated on.

In the following, we will focus on the case $M = 2$, which is relevant e.g. in an uplink-downlink scenario. While the study can be extended to $M > 2$, an increase in M will render the processing of the decision variables mathematically more complicated. As will be seen, the probability of false alarm and detection expressions are not trivial even for $M = 2$,

[1] We note that the assumption of a frequency nonselective channel is not critical for our studies.

[2] Accordingly, the corresponding active and inactive systems can be determined using the subscript of p_i in (8).

and can only be evaluated using numerical integration. Hence, for $M > 2$ there will be possibly more interdependent links and determining the optimum detection values will be much more challenging. Therefore, in this study we only consider the practical case of $M = 2$, and leave the case $M > 2$ as a subject for further investigation.

III. Joint Detection

For detection of the primary system, it is assumed that the systems' joint activity values $\{p_i\}$ and the pdfs of the decision variables $\{d_m\}$ are known a priori. This is a reasonable assumption as the traffic information of the primary systems may be available to secondary users, and the SNR of the primary signals can be estimated at the UWB receiver. Since $\{p_i\}$ and $\{d_m\}$ are known, the MAP decision rule can be employed for joint detection. Accordingly, the hypothesis can be estimated by finding the maximum of the MAP decision metrics as

$$\hat{i} = \arg\max_{i\in\{0,1,2,3\}} PM_i$$
$$\hat{\mathbf{H}} = \mathbf{H}_0 \text{ if } \hat{i} = 0; \quad \hat{\mathbf{H}} = \mathbf{H}_1 \text{ if } \hat{i} = \{1,2,3\} \tag{9}$$

where $PM_i = b_i p_i f_{D_1,D_2|\mathbf{H}_{1,i}}(d_1,d_2)$, $\{i=1,2,3\}$, $PM_0 = b_0 p_0 f_{D_1,D_2|\mathbf{H}_0}(d_1,d_2)$, $\{b_i \,|\, i = 0,1,2,3\}$ are intentionally introduced bias terms that are used to achieve a desired trade-off between the probabilities of detection and false alarm, and $f_{D_1,D_2|\mathbf{H}_0}(d_1,d_2)$ and $f_{D_1,D_2|\mathbf{H}_{1,i}}(d_1,d_2)$ are the joint pdfs of the decision variables d_1 and d_2 conditioned on the corresponding hypothesis, respectively. Since the decision variables are obtained from non-overlapping frequency bands, the pdfs of the variables are independent. Hence, the decision metrics, $\{PM_i \,|i=0,1,2,3\}$ simplify to

$$PM_i = b_i\, p_i\, C \prod_{m=1}^{2} \frac{\exp\left(\frac{-d_m}{2(\gamma_m+1)^{x_m}}\right)}{(\gamma_m+1)^{x_m N_m/2}} \tag{10}$$

where $C = \prod_{m=1}^{2} \frac{d_m^{N_m/2-1}}{2^{N_m/2}\Gamma(N_m/2)}$ is a common term for all PM_i. Based on (9), the probabilities of false alarm and detection can be defined, respectively, as

$$P_f = 1 - \Pr\left[\bigcap_{i=1}^{3}\left(PM_0 > PM_i\right)\Big|\mathbf{H}_0\right] \tag{11}$$

$$P_d = 1 - \sum_{i=1}^{3}\frac{p_i}{1-p_0}\Pr\left[\bigcap_{j=1}^{3}\left(PM_0 > PM_j\right)\Big|\mathbf{H}_{1,i}\right]. \tag{12}$$

By substituting (10) into the comparison term $\{PM_0 > PM_i\}$, (11) and (12) can be simplified to

$$P_f = 1 - P_{\lambda_3\,|\,\lambda_1,\lambda_2,\mathbf{H}_0}\left[\prod_{m=1}^{2}(1-P_{f,m})\right] \tag{13}$$

$$P_d = 1 - \sum_{i=1}^{3}\frac{p_i}{1-p_0}P_{\lambda_3\,|\,\lambda_1,\lambda_2,\mathbf{H}_{1,i}} \cdot \left[\prod_{m=1}^{2}(1-P_{d,m})^{x_m}(1-P_{f,m})^{(1-x_m)}\right] \tag{14}$$

where $P_{\lambda_3\,|\,\lambda_1,\lambda_2,\mathbf{H}_x}$, $\{x=0\}$ or $\{x=1,i\}$, is the conditional probability term obtained as

$$P_{\lambda_3\,|\,\lambda_1,\lambda_2,\mathbf{H}_x} = \Pr\left[\sum_{m=1}^{2} d_m a_m < \lambda_3 \Big| d_1<\lambda_1, d_2<\lambda_2, \mathbf{H}_x\right] \tag{15}$$

with $\lambda_m = \left[\frac{N_m}{2}\ln\left(\gamma_m+1\right) + \ln\left(\frac{p_0}{p_m}\right) + \ln\left(\frac{b_0}{b_m}\right)\right] \Big/ a_m$ and $a_m = \frac{\gamma_m}{2(\gamma_m+1)}$ for $m = \{1,2\}$, and the threshold $\lambda_3 = \left[\sum_{m=1}^{2}\frac{N_m}{2}\ln\left(\gamma_m+1\right) + \ln\left(\frac{p_0}{p_3}\right) + \ln\left(\frac{b_0}{b_3}\right)\right]$. The conditional probability term depends on the value of λ_3 and can be expressed as

$$\begin{aligned} P_{\lambda_3\,|\,\lambda_1,\lambda_2,\mathbf{H}_x} &= \int_0^{\lambda_3/a_1} f_{D_1}(d_1)\int_0^{-\frac{a_1}{a_2}d_1+\frac{\lambda_3}{a_2}} f_{D_2}(d_2)\,\mathrm{d}d_2\,\mathrm{d}d_1 \\ &\quad - \int_{\lambda_1}^{\lambda_3/a_1} f_{D_1}(d_1)\int_0^{-\frac{a_1}{a_2}d_1+\frac{\lambda_3}{a_2}} f_{D_2}(d_2)\,\mathrm{d}d_2\,\mathrm{d}d_1 - \int_{\lambda_2}^{\lambda_3/a_2} f_{D_2}(d_2)\int_0^{-\frac{a_2}{a_1}d_2+\frac{\lambda_3}{a_1}} f_{D_1}(d_1)\,\mathrm{d}d_1\,\mathrm{d}d_2 \\ &= A_1 - A_2 - A_3\,. \end{aligned} \tag{16}$$

Each term can be simplified and computed using numerical integration as

$$A_1 = \int_0^{\lambda_3/a_1} f_{D_1}(d_1)\left[1 - Q\left(\frac{N_2}{2}, \left(-\frac{a_1}{a_2}d_1 + \frac{\lambda_3}{a_2}\right)\Big/\sigma_2^2\right)\right]\mathrm{d}d_1 \tag{17}$$

$$A_3 = \int_{\lambda_2}^{\lambda_3/a_2} f_{D_2}(d_2)\left[1 - Q\left(\frac{N_1}{2}, \left(-\frac{a_2}{a_1}d_2 + \frac{\lambda_3}{a_1}\right)\Big/\sigma_1^2\right)\right]\mathrm{d}d_2 \tag{18}$$

where term A_2 is the same as A_1 but with the integration interval changed from $[0, \frac{\lambda_3}{a_1}]$ to $[\lambda_1, \frac{\lambda_3}{a_1}]$. Note that depending on the values of $\{\lambda_1,\lambda_2,\lambda_3\}$, the integration intervals of A_2 and A_3 may not exist, hence, A_2 and A_3 may be equal to 0.

Consider the probabilities of false alarm and detection given in (13) and (14). If the conditional probability terms $\{P_{\lambda_3\,|\,\lambda_1,\lambda_2,\mathbf{H}_x}\}$ are equal to unity, then the expressions simplify to the conventional probability expressions for independent detection. Accordingly, depending on the value of λ_3, both of the values in the (P_f, P_d)-pair obtained from (13) and (14) will be no less than the values in the (P_f, P_d)-pair obtained from independent detection. In other words, since independent detection is a special case of joint detection, the receiver operating characteristic (ROC) performance of the latter is superior for properly chosen thresholds. We will now present two methods to determine the $(\lambda_1,\lambda_2,\lambda_3)$-triplets[3] for joint detection.

A. Optimal Joint Detection

In order to obtain the best detection performance, the NP test can be used. Accordingly, P_d can be maximized by optimizing the threshold values $\{\lambda_1,\lambda_2,\lambda_3\}$ jointly for a target probability of false alarm $P_f = \alpha$. This can be formulated as

$$\max_{\lambda_1,\lambda_2,\lambda_3} \; P_d \quad s.t. \quad P_f = \alpha. \tag{19}$$

To obtain the $(\lambda_1,\lambda_2,\lambda_3)$-triplet that maximizes the P_d value for a target $P_f = \alpha$ value, (6), (7), (13), and (14) should

[3]Once the $(\lambda_1,\lambda_2,\lambda_3)$-triplets are determined, the bias values $\{b_i\}$ can be obtained from $\{\lambda_m\}$ given after (15) for the practical implementation of the MAP decision rule.

be used in (19). This is achieved by initially finding the $(\lambda_1, \lambda_2, \lambda_3)$-triplets that satisfy the constraint, then calculating P_d over the complete set of $(\lambda_1, \lambda_2, \lambda_3)$-triplets, and finally selecting the $(\lambda_1, \lambda_2, \lambda_3)$-triplet that maximizes the P_d value. By letting $P_f = \alpha$ in (13), the λ_3-value that satisfies the conditional probability for given λ_1 and λ_2 values can be obtained from

$$P_{\lambda_3 \mid \lambda_1, \lambda_2, \mathbf{H}_0} = \frac{1-\alpha}{\left(1-Q\left(\frac{N_1}{2}, \frac{\lambda_1}{2}\right)\right)\left(1-Q\left(\frac{N_2}{2}, \frac{\lambda_2}{2}\right)\right)} \leq 1 . \quad (20)$$

For every (λ_1, λ_2)-pair, $P_{\lambda_3 \mid \lambda_1, \lambda_2, \mathbf{H}_0}$ given in (16)–(18) is calculated by varying the λ_3-value in order to satisfy (20) given above. The obtained $(\lambda_1, \lambda_2, \lambda_3)$-triplets that satisfy the $P_f = \alpha$ constraint are then used in (14) to find the $(\lambda_1, \lambda_2, \lambda_3)$-triplet that maximizes P_d. The process for finding the $(\lambda_1, \lambda_2, \lambda_3)$-triplets is computationally complex since the λ_3-values are calculated iteratively from $P_{\lambda_3 \mid \lambda_1, \lambda_2, \mathbf{H}_0}$ for the large set of possible $\{\lambda_1, \lambda_2\}$-values. Alternatively, we consider a suboptimal method for joint detection.

B. Suboptimal Joint Detection

The $\{\lambda_m\}$ values given after (15) result from the corresponding $\{PM_0 > PM_m\}$ comparisons for $m = \{1, 2, 3\}$, and are used in determining the probabilities of false alarm and detection given in (13) and (14). When $b_0 = b_1 = b_2 = b_3$, $\ln(\frac{b_0}{b_m}) = 0 \ \forall m$ in $\{\lambda_m\}$, and the MAP detection minimizes the probability of error; i.e., $P_e = p_0 P_f + (1-p_0)(1-P_d)$ is minimized. On the other hand, depending on the coexistence requirements between primary and secondary users, the probability of false alarm, P_f, and the probability of missdetection, P_{md}, can be traded off. This is achieved by varying the bias values $\{b_m\}$ in $\{\lambda_m\}$. By letting $b_1 = b_2 = b_3 = b$, the complementary ROC curve can be generated by only varying b of the bias term $\ln(\frac{b_0}{b})$ in $\{\lambda_m\}$ $\forall m$. This assumption significantly reduces the computational complexity for obtaining the (P_f, P_d)-pairs compared to the NP test for joint detection, and yet the detection performance is found to be very close to that for the NP test based detection. In Fig. 1, the suboptimal joint detection is numerically evaluated using (13) and (14) with the condition $b_1 = b_2 = b_3 = b$ in $\{\lambda_m\}$, and verified by simulating the decision metrics in (10) and evaluating them in (11) and (12) for two different sets of system parameters. In addition, suboptimal and optimal joint detection methods are compared. By letting $P_f = \{10^{-1}, 10^{-2}, 10^{-3}, 10^{-4}\}$ possible $(\lambda_1, \lambda_2, \lambda_3)$-triplets are calculated, and the corresponding P_{md} values obtained by the NP test and the minimum P_{md} values for each P_f value are plotted for comparison. It can be observed that the minimum P_{md} values obtained by the NP test coincide with the ROC curve of the suboptimal detection. Due to its simple computation and close-to-optimal performance, we will adopt the suboptimal joint detection approach for performance comparison with independent detection in the next section.

IV. Numerical Results

In this section, the gains of joint detection over independent detection are evaluated for various scenarios. The corresponding complementary ROC curves are obtained by

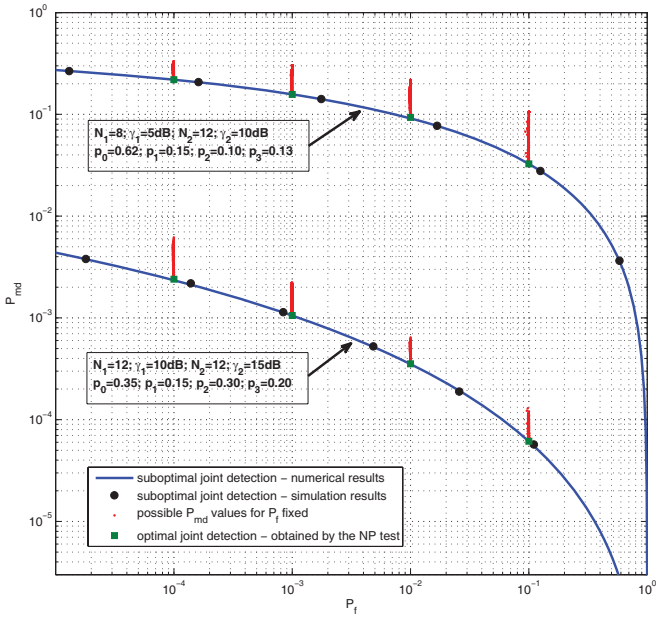

Fig. 1. Complementary ROC curves of suboptimal and optimal joint detection for two different sets of system parameters.

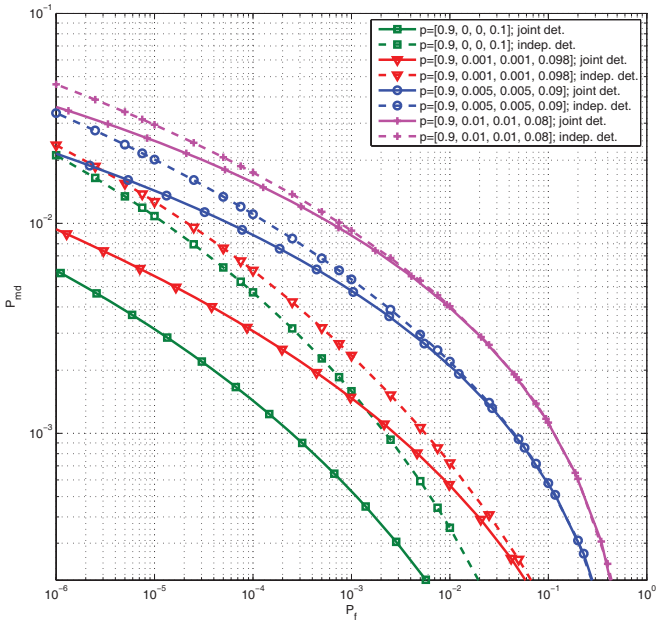

Fig. 2. The effect of system activity values on the detection performances when $N_1 = N_2 = 8$ and $\gamma_1 = \gamma_2 = 10$ dB.

the suboptimal joint detection approach and the optimal NP test based independent detection.

In Fig. 2, joint and independent detection are compared for various $\mathbf{p}$ values when $N_1 = N_2 = 8$ and $\gamma_1 = \gamma_2 = 10$ dB. The common property of the $\mathbf{p}$ values in the legend of Fig. 2 is that they all satisfy $\Pr[\mathbf{H}_0] = 0.90$ and $\Pr[\mathbf{H}_1] = 0.10$, i.e., the primary system is active 10% of the time. The case when $\mathbf{p} = [0.9\ 0\ 0\ 0.1]$, where the uplink and downlink are fully dependent, serves as a benchmark for the detection gain of joint detection over independent detection. Accordingly, it is observed that the detection gain of joint detection decreases

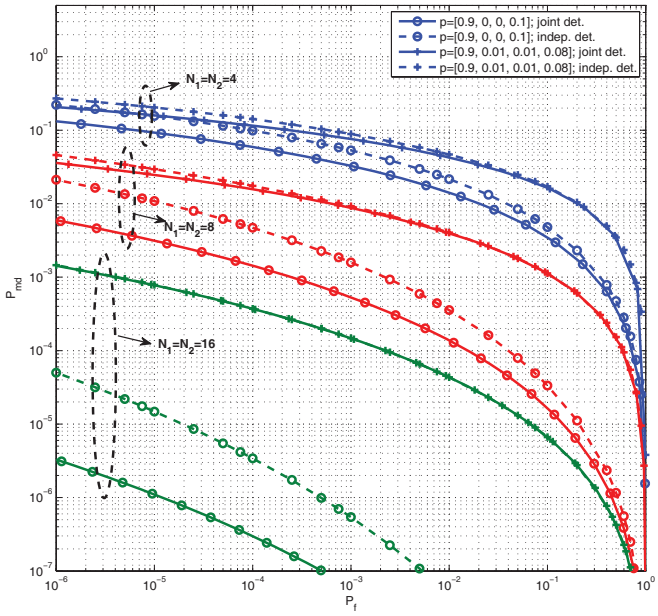

Fig. 3. The effect of the integration time on the detection performances when $\gamma_1 = \gamma_2 = 10$ dB is fixed and $N_1 = N_2 = \{4, 8, 16\}$ for two sets of system activity values.

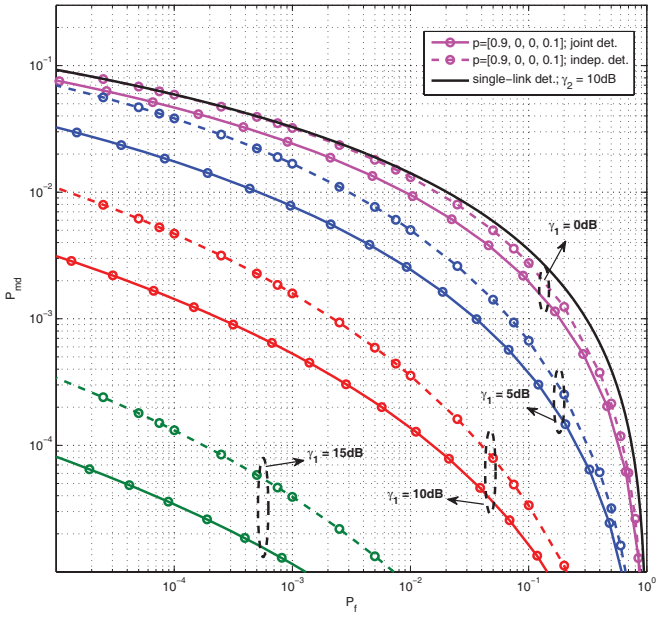

Fig. 4. Complementary ROC curves for simultaneous uplink-downlink communication when the uplink SNR is constant and the downlink SNR is varying.

with decreasing p_3 values for fixed $\Pr[\mathbf{H}_1] = 0.10$. It can also be observed that the detection gain of joint detection is larger for low values of P_f.

In Fig. 3, the effect of integration time on the detection performances is investigated when $\gamma_1 = \gamma_2 = 10$ dB is fixed and $N_1 = N_2 = \{4, 8, 16\}$ for system activity values $\mathbf{p} = [0.9\ 0\ 0\ 0.1]$ and $\mathbf{p} = [0.9\ 0.01\ 0.01\ 0.08]$. The selection of $N_1 = N_2$ indicates that both links have the same bandwidth $W_1 = W_2$ and the same receiver integration times $T_1 = T_2$. We can observe from Fig. 3 that the P_{md} of independent detection is about three times the P_{md} of joint detection at $P_f = 10^{-4}$ for $N_1 = N_2 = 8$ when the links are fully dependent. By doubling the integration time (i.e., $N_1 = N_2 = 16$), the performance gain can be increased ten-fold.

In Fig. 4 we consider the detection of a system with simultaneous uplink-downlink communications when the uplink SNR is constant and the downlink SNR is varying. The complementary ROC curves are plotted when $\gamma_2 = 10$ dB, $\gamma_1 = \{0, 5, 10, 15\}$ dB, $N_1 = N_2 = 8$, and $\mathbf{p} = [0.9\ 0\ 0\ 0.1]$. As expected, both joint and independent detection performances improve and the gain of joint detection increases with γ_1. When the downlink SNR is very low (i.e., $\gamma_1 = 0$ dB), the performance of independent detection over two links becomes equivalent to the performance of the single-link detection of the uplink for low P_f values. On the other hand, the probability of missdetection for joint detection is about 30% less compared to the independent detection at $P_f = 10^{-3}$ when $\gamma_1 = 0$ dB. This can be explained by the efficient processing of decision variables obtained from both links.

We now consider the uplink-downlink scenario when the UWB-IR is far from the downlink operation (i.e., low SNR) and there is downloading most of the time (i.e., link with low SNR is more active). Since the links are not jointly active most of the time, the performances of independent and joint detection are very close, hence, only the results of joint detection are plotted. In Fig. 5, the effect of integration time on the detection performance is investigated when $\gamma_1 = 5$ dB (downlink) and $\gamma_2 = 10$ dB for various system activity values. For all cases, it is assumed that $\Pr[\mathbf{H}_0] = 0.90$ and $\Pr[\mathbf{H}_1] = 0.10$ for a fair comparison. The case $N_1 = N_2 = 8$ serves as a benchmark. When $p_1 = 0.08$, i.e., only the downlink is active 80% of the time when the system is active, the performances are the worst due to the low SNR of the highly active link. When $p_1 = 0.04$, the performances improve, and the detection performance is the best for $\mathbf{p} = [0.9\ 0.04\ 0\ 0.06]$, where the links are jointly

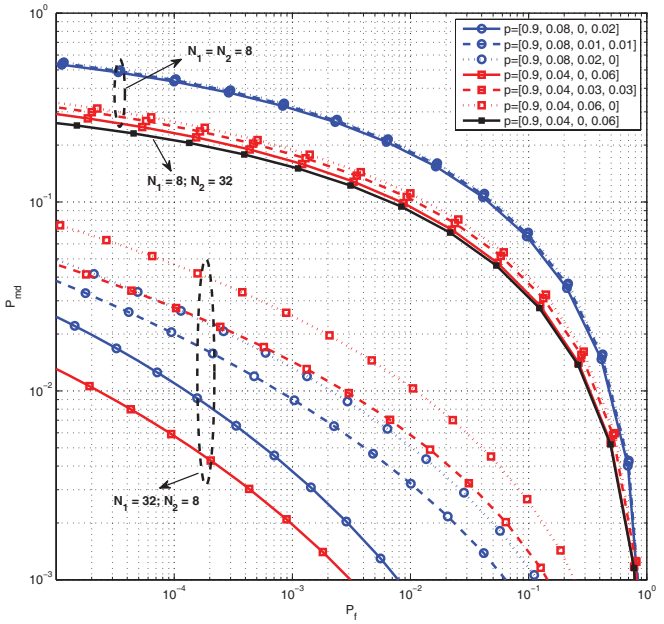

Fig. 5. The effect of integration time on the detection performances when downlink with low SNR is more active.

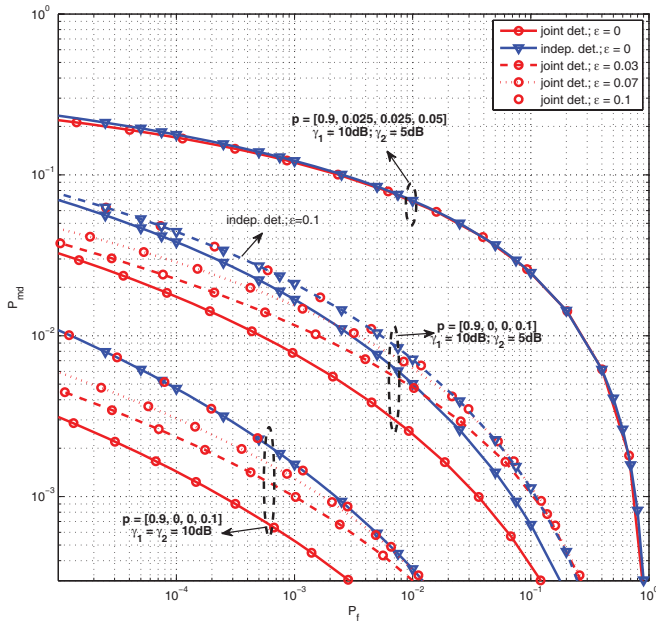

Fig. 6. The effect of imperfect knowledge of the system activity values on the detection performances for various system parameters.

active most of the time. When the integration time for uplink, i.e., N_2, is increased, the performances for different activity values do not change significantly. On the other hand, when the integration time for downlink is increased, all the performances significantly improve with $\mathbf{p} = [0.9\ 0.04\ 0\ 0.06]$ having the best performance.

Finally, we consider the effect of imperfect knowledge of the system activity values on the detection performances in Fig. 6. The estimated system activity values are $\hat{\mathbf{p}} = [p_0 \quad p_1+\epsilon/2 \quad p_2+\epsilon/2 \quad p_3-\epsilon]$, where ϵ determines the error. It is assumed that $N_1 = N_2 = 8$ for all cases. When there is simultaneous uplink-downlink communication with equal SNR, $\gamma_1 = \gamma_2 = 10$ dB, the joint detection performance degrades with ϵ. On the other hand, independent detection is not affected by ϵ due to the symmetry of the links (i.e., $N_1 = N_2$ and $\gamma_1 = \gamma_2$). Joint detection performs at least the same as independent detection even when the estimation error is large. When $\gamma_1 = 10$ dB and $\gamma_2 = 5$ dB, i.e., the links are not symmetric anymore, independent detection also degrades. When the performances are compared, joint detection with $\epsilon = 0.03$ still outperforms independent detection with no estimation error for P_f values of less than 10^{-2}. When the system activity values are $\mathbf{p} = [0.9\ 0.025\ 0.025\ 0.05]$, independent and joint detection schemes perform similar with almost no performance degradation observed for various ϵ values.

V. Conclusion

In this study, the primary system detection performance of UWB-IR systems was investigated assuming that the primary systems are potentially dependent. Contrary to selecting the detection thresholds individually for each band as in the conventional detection approach, we considered processing the bands jointly based on the MAP decision rule. For the joint detection, both the optimal NP test based detection and a suboptimal but practically implementable approach were considered. This study shows that joint detection outperforms independent detection significantly (i) if the systems are jointly active most of the time as in simultaneous uplink-downlink communication, (ii) for the low probability of false alarm ROC region, and (iii) when the SNR and receiver integration times in each band are large enough. The results obtained from this study are important for the improvement of the detection performance of UWB-IRs and cognitive radios.

References

[1] IEEE Std 802.15.4a-2007, "Part 15.4: Wireless Medium Access Control (MAC) and Physical Layer (PHY) Specifications for Low-Rate Wireless Personal Area Networks (WPANs)," 2007.

[2] European Commission, "2009/343/EC: Commission Decision of 21 April 2009 amending Decision 2007/131/EC on allowing the use of the radio spectrum for equipment using ultra-wideband technology in a harmonised manner in the Community," *Official Jour. of European Union*, L 109/9–13, Apr. 2009.

[3] F. F. Digham, M.-S. Alouini, and M. K. Simon, "On the energy detection of unknown signals over fading channels," *IEEE Trans. Commun.*, vol. 55, pp. 21–24, Jan. 2007.

[4] A. Pandharipande and J.-P. M. G. Linnartz, "Performance analysis of primary user detection in a multiple antenna cognitive radio," in *Proc. IEEE ICC '07*, pp. 6482–6486, June 2007.

[5] Y.-C. Liang, Y. Zeng, E. C. Y. Peh, and A. T. Hoang, "Sensing-throughput tradeoff for cognitive radio networks," *IEEE Trans. Wireless Commun.*, vol. 7, pp. 1326–1337, Apr. 2008.

[6] S. M. Mishra and R. W. Brodersen, "Cognitive technology for improving ultra-wideband (UWB) coexistence," in *Proc. IEEE ICUWB '07*, pp. 253–258, Sep. 2007.

[7] K. Ohno and T. Ikegami, "Interference DAA technique for coexisting UWB radio," in *Proc. IEEE VTC-Spring '07*, pp. 2910–2914, Apr. 2007.

[8] S. Erküçük, L. Lampe, and R. Schober, "Analysis of interference sensing for DAA UWB-IR systems," in *Proc. IEEE ICUWB '08*, vol. 3, pp. 17–20, Sep. 2008.

[9] Z. Quan, S. Cui, A. H. Sayed, and H. V. Poor, "Optimal multiband joint detection for spectrum sensing in cognitive radio networks," *IEEE Trans. Signal Process.*, vol. 57, pp. 1128–1140, Mar. 2009.

[10] M. Abramowitz and I. Stegun, *Handbook of Mathematical Functions*. New York: Dover, 1964.